

# The effect of fibre sizing on fibres and bundle strength in hybrid glass carbon fibre composites

C. MARSTON, B. GABBITAS\*, J. ADAMS

*School of Engineering Systems Design, South Bank University, London SE1 0AA, UK*

Tests have been carried out on single carbon fibres supplied in the sized and unsized conditions, as well as impregnated tows and tows in a glass–carbon fibre hybrid composite of the same fibre. The results were analysed using a Weibull distribution for the strengths of the reinforcing fibres and composites. The tensile strength of the single fibres appeared to be unaffected by the sizing of the filaments. In the case of the impregnated tows, an increase in characteristic strength of 7% was observed for the unsized fibres. The strength of the impregnated tows in hybrid composites was seen to be 15% higher than those tested in air. This can be attributed to the “hybrid effect”.

## 1. Introduction

The ability of the interface to transfer stress in fibrous composites is known to play an essential role in their performance. In order to explain the shear properties of composite systems, the assumption is often made that an intermediate layer exists between the fibre and the matrix which is referred to as the interphase. In thermoplastic matrix composites the interphase has clearly been identified [1] and may be promoted by the presence of a coupling agent such as fibre sizing between the fibre and the matrix. It is common practice to coat the fibres after production with a layer of protective size. The sizing on carbon fibre usually consists of a thin layer of usually epoxy resin which protects the carbon fibre surface and enhances the interfacial properties. Guignon and Klinklin [2] have shown that the different sizings may improve the interfacial properties, but if the sizing is not compatible with the matrix, there is decohesion at the sizing/matrix interface. Cheung *et al.* [3] conducted a detailed study of the sizing effect using both commercial and experimental sizings. They reported a dependence of the stress-transfer efficiency on molecular weight, deposition procedure, as well as, in some cases, on the presence of an interphase region as manifested by SEM studies. Yumitory *et al.* [4] reported that the presence of a sizing resin improves the interface of a PES thermoplastic matrix composite but tends to the creation of the weak interphase in the case of epoxy matrix systems. In conclusion, it seems that the presence of sizing in carbon fibre/polymer interfaces plays an important role in the properties of the interface but as yet its effect upon the strength of a composite has not been adequately quantified.

If the strength of a composite is expressed in terms of the strengths of its components according to the simple law of mixtures, it is implicitly assumed that the

strength of the fibres are all the same. This is oversimplistic and in a practical composite this assumption is not valid. Thus, in a fully descriptive model of the tensile strength, many factors must be considered. For example, the variability of the fibre strength is known to be determined by the distribution of flaws and can be described by a “weak link” principle. Also of concern is the neighbouring surviving fibres adjacent to a break which will be subject to a stress concentration,  $K_r$ , over a positively affected length [5]. This stress overload increases the probability that a neighbouring fibre will fail. The stress concentration factor,  $K_r$ , is related to the interfibre distance, the fibre/matrix properties, the number of broken fibres (cluster size) and the ineffective length. The ineffective length depends upon the strength of the fibre/matrix bond, thus the fracture characteristics in a composite can be modified by careful control of the interface.

The most established models for the failure of simple-uniaxial composites are based on the application of Weibull statistics [6]. The strength of the single fibre, randomly sampled from a yarn and uniformly loaded over a gauge length  $L_0$ , is assumed to follow a Weibull distribution of the form

$$P_{f(s)} = \left[ 1 - \exp\left(-\frac{\sigma}{\sigma_0}\right)^w \right] \quad (1)$$

where  $\sigma$  is the applied stress,  $\sigma_0$  is the characteristic stress at unit length and  $w$  is the shape parameter. As described by Watson and Smith [7], the scaling of strength with gauge length is embodied in the Weibull scale parameter through the relationship

$$\sigma_L = \sigma_0 \left(\frac{L_0}{L}\right)^{1/w} \quad (2)$$

\*Author to whom all correspondence should be addressed.

where  $\sigma_L$  and  $L$  are the strength and length of the segment,  $\sigma_0$  is the measured strength at a reference length  $L_0$  and  $w$  is the Weibull shape parameter.

The objective of this work was to assess the effect of sizing upon the strength of single fibres, impregnated tows and glass-carbon fibre hybrid composites. The term “hybrid composite” is used to describe more than one type of fibre material, and in this study tows, in a hybrid glass laminate, are prepared. The impregnated tow had a lower strain to failure than the glass-reinforcing matrix, thus the effect of fibre sizing upon the failure mechanism can be investigated.

## 2. Experimental procedure

### 2.1. Single-fibre tests

Sized (MEBS) M40B-6K-40B and unsized (MUS) M40B-6K-40B carbon fibres supplied by Soficar (Soficar (Toray) Industries, France) were used in this study. The fibres were 6.6  $\mu\text{m}$  in effective diameter [8].

Single fibres were peeled from the tow and then mounted by means of a cyanoacrylate glue on window card types designated in ASTM (D3379) [9]. The typical specimen mounting geometry is shown in Fig. 1a. The tensile strength of single fibres from each batch were measured using an Instron 4507 machine.

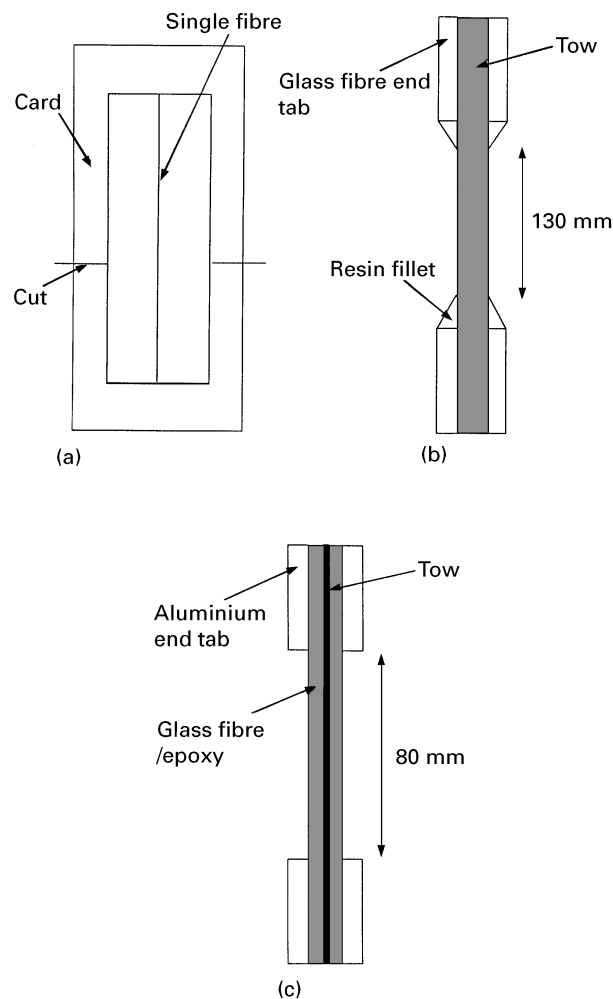


Figure 1 Schematic illustration of the specimen geometry: (a) single-fibre specimen mounting, (b) impregnated tow, (c) hybrid bundle.

Approximately 55 measurements were made using fibres with a gauge length of 40 mm for each batch. The average fibre diameter was measured by a technique based on the density of fibres [8]. The system compliance was determined experimentally for the Instron test machine and grip systems, because the specimen brittleness prevented the use of a normal strain-sensing device.

In addition, fibres of different gauge lengths (10, 25, 50 mm) were tested by Favre *et al.* [8]. As before, fibres were mounted on window cards and tensile failure stresses of the fibres were obtained. Approximately 30 tests were carried out for each gauge length and was analysed according to the Weibull distribution.

### 2.2. Impregnated tow test

Single tows of 6000 sized and unsized fibres were impregnated with a two-part LY-HY 5052 Ciba-Geigy (Ciba-Geigy, Cambridge, UK) epoxy resin. The LY-HY 5052 resin is based on epoxy novolac and difunctional reactive diluent. The HY 5052 hardener was based on cycloaliphatic amine with phenolic accelerator and organic acid accelerator present. Specimens were prepared by pulling the tows from the spool through a resin bath at room temperature, then through a 0.4 mm die to improve consolidation and control the fibre volume fraction. The resulting material was a cylindrical rod of composite, approximately 0.4 mm diameter, with a fibre volume fraction of 55%–60%. A schematic illustration of the impregnated tow test piece is shown in Fig. 1b. Impregnated tows were prepared for tensile testing by fitting braided tabs. Approximately 40 impregnated bundle specimens of sized and unsized fibres at a gauge length of 130 mm were strained on the testing rig as before.

In order to investigate the build-up of fibre breaks during axial tension, some of the tows were tested to pre-selected stress levels. The damage was then analysed by sectioning three 20 mm lengths of the sample longitudinally for each level of applied strain. The number of individual breaks or singlets, plus the fibre breaks adjacent to these singlets, referred to as *i*-plets by Batdorf [10], were counted using a light microscope. The number of fibres transversed when travelling across the specimen width multiplied by the length of a section gives an indication of the length of fibre studied. For comparative purposes the number of *i*-plets observed was scaled to *i*-plets per meter.

### 2.3. Hybrid bundle tests

These specimens were made by incorporating a single impregnated tow into a uniaxial glass-fibre/epoxy resin. These specimens preserved the failure zone of the tows. E-glass fibre rovings were laid onto a 200 mm square aluminium frame with 10 rods of impregnated tow laid at intervals of 20 mm. Precautions were taken to ensure that the carbon tows remained straight and parallel to the glass rovings. To maintain alignment of the glass fibres, tension was applied to the filaments by attaching them to the frame

with adhesive tape. The glass fibre and tows were impregnated with the LY-HY 5052 resin and cured by placing the mould in a press. The hybrid composite was cut into 15 mm by 80 mm coupons ensuring that the carbon tow was centrally located at the specimen mid-width, as shown by the schematic illustration in Fig. 1c. Aluminium end tabs were attached to the hybrid composite sample using an epoxy adhesive and left to cure overnight. Ten hybrid composite samples were tested in tension using an Instron 4507 tensile testing machine. Owing to the transparency of the epoxy resin/glass fibre, failures in the composite tow could be observed with the naked eye. The hybrid samples were strained until the first impregnated tow failure was observed. The hybrid composite failure site was prepared for microscopic examination by metallographic polishing on a rotary grinding machine.

### 3. Results

#### 3.1. Single-fibre and bundle-strength distributions

A summary of Weibull modulus,  $w$ , and the characteristic strength,  $\sigma_0$ , for failure stress of the sized and unsized single fibres, impregnated tows and hybrid composite is shown in Table I. In the case of the single fibres, the Weibull modulus ranged from 6.7–13.2, representing a fairly wide range of scatter. The characteristic strength is observed to increase from 2864 MPa to 3294 MPa as the fibre gauge length decreases from 50 mm to 10 mm for the sized fibres. The sized fibre strength increases from 2807 MPa to 3395 MPa as the gauge length decreases from 40 mm to 10 mm, with the 50 mm single-filament data being inconsistent with this trend.

The characteristic strength of a fibre at any different specified length may be calculated using the weak-link scaling principle shown in Equation 2. A “master curve” that scales the single-fibre data for the different gauge lengths into one gauge length of 40 mm is shown in Fig. 2a and b for the MUS and MEBS filaments, respectively. The proximity of the data to

a straight line (except for the tail variations), indicates the applicability of Weibull statistics to the filament data set. Weibull modulus values of 7.8 and 8.4 and characteristic strength values of approximately 2980 MPa were recorded for both the MEBS and MUS single filaments, respectively.

Fig. 3a and b shows the strength results for the 40 impregnated MUS and MEBS tow specimens tested at a gauge length of 130 mm on a Weibull plot. The values of Weibull modulus of 15.0 and 18.2 for the MEBS and MUS fibres show that there was relatively little variability in the strength between the respective individual tows. Characteristic strength for failure of 1790 MPa (MEBS) and 1919 MPa (MUS) indicate a 7% increase in strength for the unsized fibre impregnated tows.

In the hybrid samples, individual tow failures were observed as sudden discrete events. The position of the tow failure was seen through the transparent glass/epoxy. The data from the unsized and sized tow 80 mm hybrid composites are plotted on a Weibull plot as shown in Fig. 4a and b, respectively. Characteristic stresses,  $\sigma_0$ , of 2090 and 2220 MPa are recorded for the sized and unsized fibres, respectively. The Weibull modulus was found to be, respectively, 30.8 and 25.1 for the MEBS and MUS hybrid impregnated tows. It is possible to compare the characteristic strength at 130 mm with that predicted by weakest link scaling (Equation 2) of the 80 mm gauge length data. Characteristic strengths of 2057 and 2177 MPa are predicted for the MEBS and MUS impregnated bundles at a 130 mm gauge length. The failure of the tow hybrid composites are seen to occur at approximately 15% higher stress than the tows tested in air.

#### 3.2. Impregnated tow failure mechanism

The impregnated tows show classic elastic/brittle failure characteristics. There was no deviation from linearity in the behaviour in the force versus displacement trace with linear elastic behaviour up to fracture. When failure occurred the tows often split

TABLE I A summary of the Weibull modulus,  $w$ , and the characteristic strength,  $\sigma_0$ , for failure stress of the sized and unsized fibre recorded for the single fibres, impregnated tows and hybrid composite

Sample	Surface treatment	Gauge length (mm)	No. of observations	Characteristic strength, $\sigma_0$ (MPa)	Weibull parameter, $w$
Single fibres	Sized	10	24	3294	6.7
		25	32	3118	13.2
		40	53	3071	8.6
		50	27	2864	6.9
		Scaled to 40	138	2980	7.8
	Unsized	10	28	3395	8.3
		25	41	3294	9.3
		40	54	2807	9.7
		50	29	3102	8.8
		Scaled to 40	152	2980	8.4
Impregnated tows	Sized	130	40	1790	15.0
	Unsized	130	40	1919	18.2
Hybrids	Sized	80	10	2090	30.8
	Unsized	80	10	2220	25.1

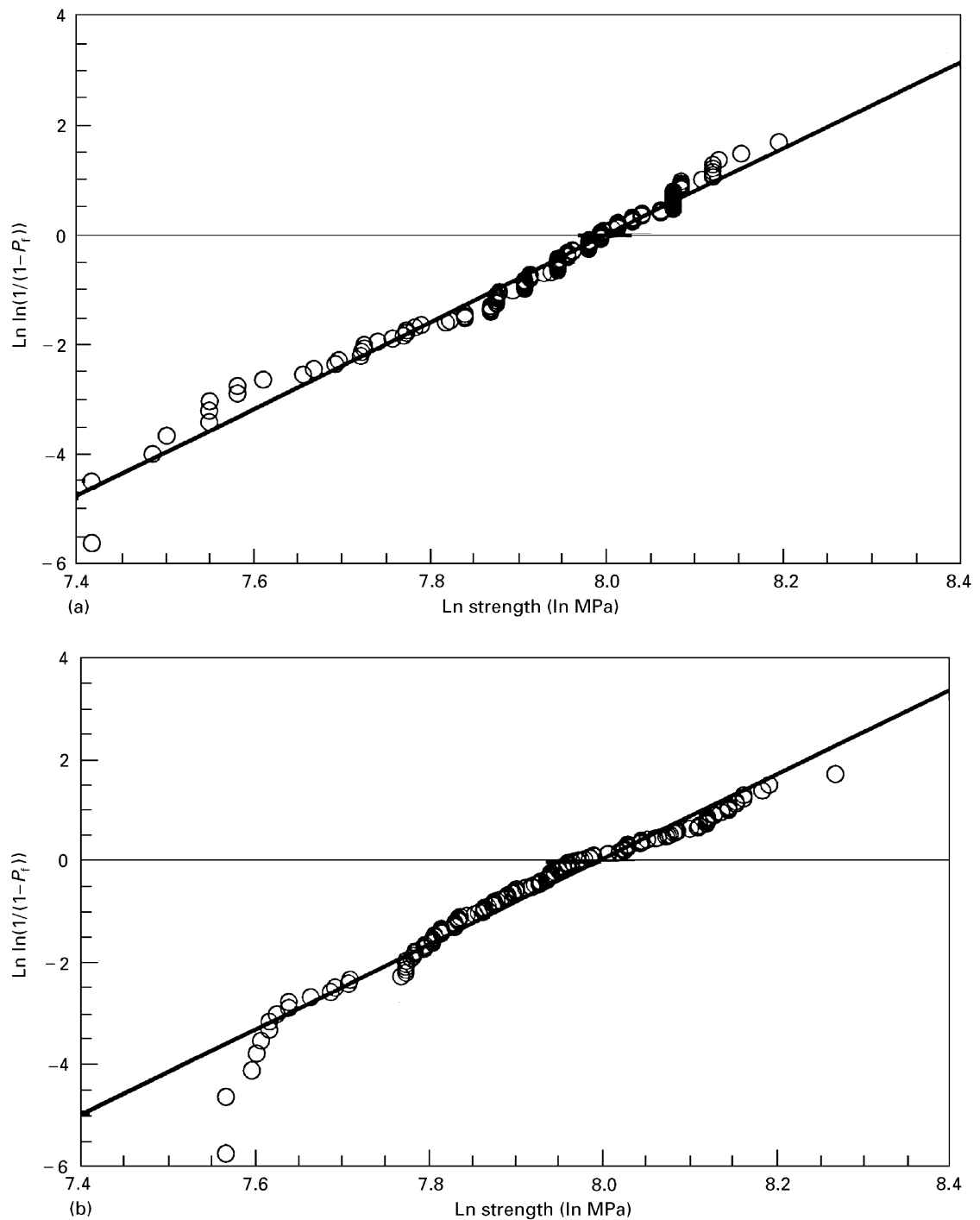


Figure 2 A Weibull plot “master curve”, scaling the data for the strength of single fibres at different gauge lengths into one gauge length of 40 mm, (a) MUS single fibres,  $w = 7.8$  (b) MEBS single fibres,  $w = 8.4$ .

into several fragments making it impossible to predict the position of the primary tensile failure.

Table II presents the results of the fibre break investigations for the MEBS and MUS tows at different levels of applied composite stress. The average number of  $i$ -plets for the three 20 mm sectioned lengths per level of applied stress are shown. In the MEBS samples the number of two-dimensional  $i$ -plets greater than one was higher than that observed in the MUS specimens. Groups of adjacent  $i$ -plets of “clusters” greater than three were observed for the MEBS tows, whereas for the MUS samples, a higher proportion of single breaks and 2-plets were seen to exist at a par-

ticular stress level. Fig. 5a and b is a photomicrograph of a two-dimensional representation of damage in the sectioned tows at an applied composite stress of 1.7 and 1.56 GPa for the MEBS and MUS tows, respectively. Fig. 5a shows the formation of single-fibre breaks in a sectioned MUS tow. Fig. 5b shows the clustering of fibre breaks for a MEBS tow. The cumulative number of filament breaks at each level of applied stress is shown in Fig. 6. The number of fibre breaks was found to increase almost exponentially for both the sized and the unsized fibre tows with few filament breaks observed at the lower levels of applied strain.

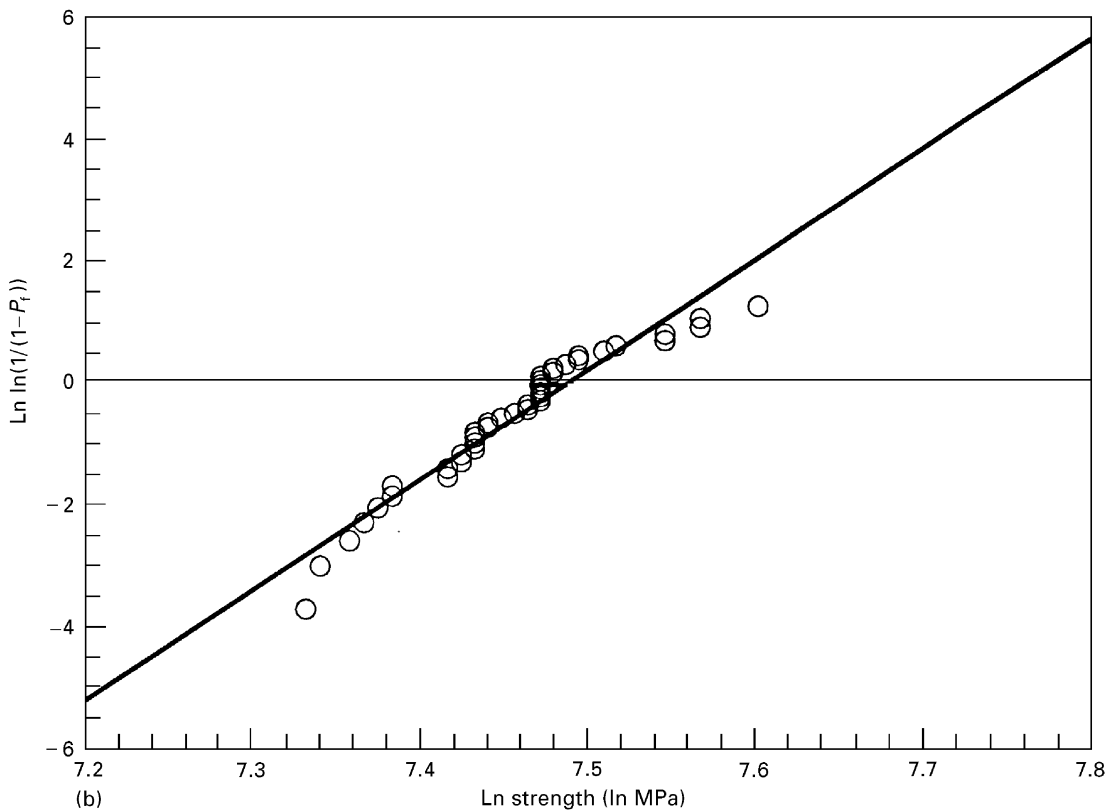
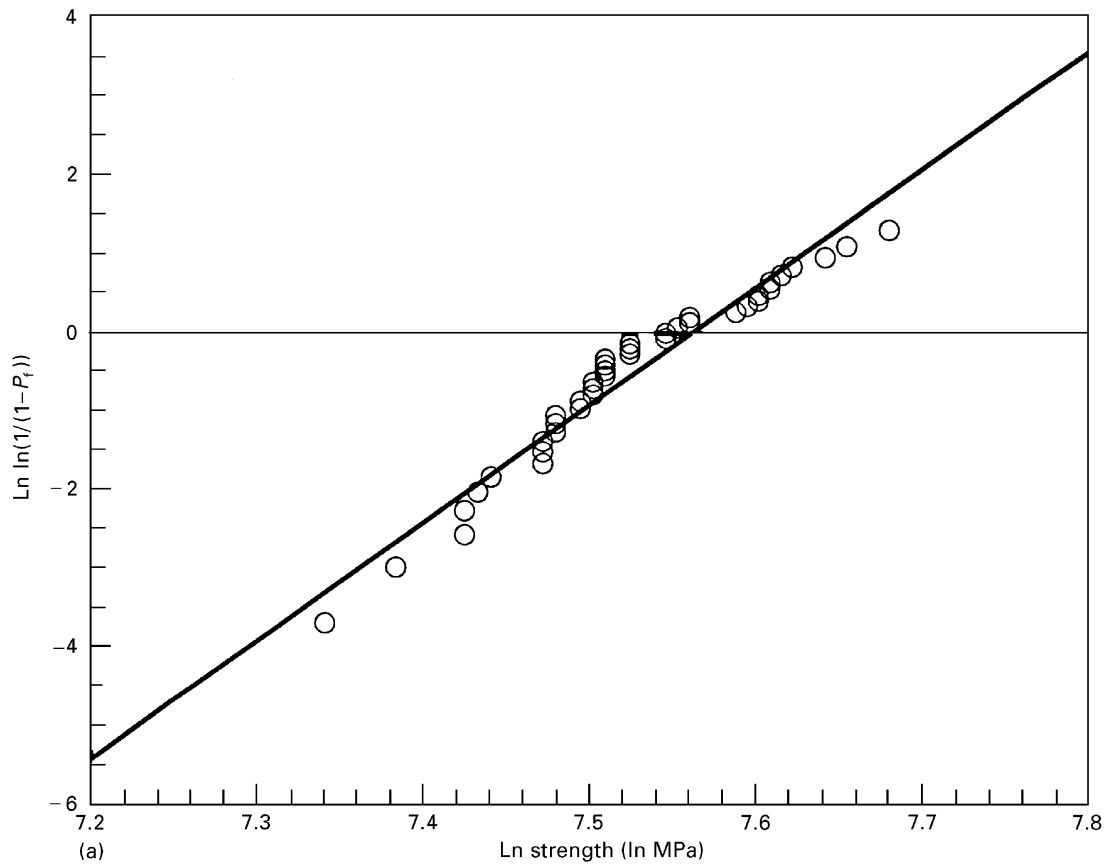


Figure 3 A Weibull plot of the strength results for the 40 impregnated tow specimens tested at a gauge length of 130 mm. (a) MUS tow,  $w = 18.2$ , characteristic strength = 1919 MPa; (b) MEBS tow,  $w = 15.0$ , characteristic strength = 1790 MPa.

Fig. 7a and b is a photomicrograph of the failure zone in a sized and unsized hybrid composite. A difference in the mode of failure was observed. In the case of the unsized tow the crack is seen to be more longitudinally extended along the fibre/matrix interface,

whereas for the sized fibre the crack propagated almost perpendicular to the fibre direction. The difference in the failure mode is attributed to the change in interfacial strength associated with the sizing of the fibre.

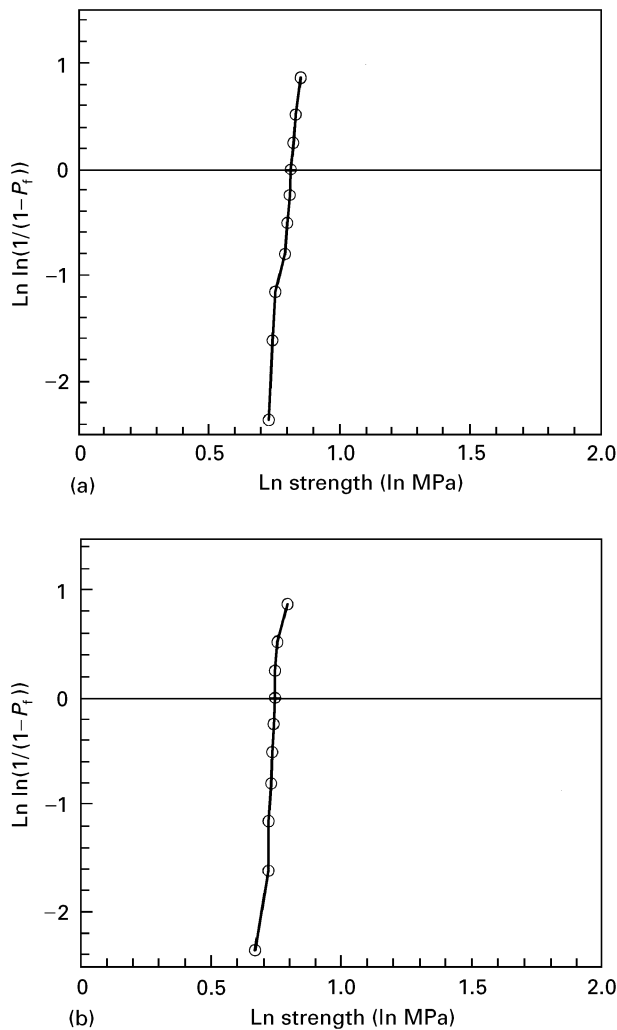


Figure 4 A Weibull plot of the strength results for the hybrid specimens tested at a gauge length of 80 mm. (a) MUS tow,  $w = 25.1$ , strength = 2220 MPa, (b) MEBS tow,  $w = 30.8$ , strength = 2090 MPa.

## 4. Discussion

### 4.1. The strength of single fibres and impregnated bundles

The characteristic strength of the single filaments was found to be relatively insensitive to the epoxy sizing

with the values for the MEBS and MUS fibre being approximately the same at the gauge length of 40 mm. However, it would be expected that the outer graphitic layers of the MUS fibres would be damaged or destroyed by abrasion during manufacture or handling. In the case of the MEBS fibres, the thin polymer sizing forms a protective layer which helps to preserve the outer graphitic layers completely intact. The “master distribution” of all the fibre strength, scaled to a 40 mm gauge length, allowed a larger data set with which to obtain the Weibull parameters.

Carbon fibres, such as those used in this study, are characterized by a variable strength which is usually attributed to the pre-existing flaws of variable size in these materials. The Weibull distributed strength has therefore, been considered, but the fibre strengths may be limited by several superimposed flaw populations as described by Anderson and Warren [11]. These populations have different flaw spacings and the apparent Weibull parameters are gauge-length dependent, as described by Zok *et al.* [12]. More importantly, test data obtained at one gauge length may be entirely misleading if extrapolated to smaller gauge length, for example in the region of the fibre ineffective length.

In the case of the impregnated tows an increase in characteristic strength of 7% is attributed to the higher interface strength associated with the sizing of the tows resulting in the clustering of fibre breaks.

The strength of the impregnated tows in the hybrid samples followed a similar trend to those tested in air, with the MUS hybrids failing at approximately 6% higher than the MEBS specimens. The hybrid bundles were approximately 15% stronger than the impregnated tows and had a higher Weibull modulus, indicating little variability in the strength of the sample. These results seem to confirm the existence of the hybrid effect, where the carbon-fibre tow is stronger when surrounded by glass fibre-reinforced material. An explanation of this higher strength has been presented by Bader and Batdorf [13]. In a smaller volume material, a surface flaw is more severe than a buried flaw. In the hybrid composite, fibre failures at the

TABLE II Fibre break investigations for the MEBS and MUS tows at different levels of applied composite stress

	Stress (GPa)	1-plets (m)	2-plets (m)	3-plets (m)	4-plets (m)	5-plets (m)	6-plets (m)	7-plets (m)
MEBS	0.6	0	0	0	0	0	0	0
	0.75	1.80	0	0	0	0	0	0
	1.09	1.53	0.16	0.16	0	0	0	0
	1.2	2.56	1.90	0.68	0.20	0	0	0
	1.34	4.53	2.00	0.4	0.63	0.20	0	0
	1.6	19.05	9.10	1.53	0.55	0.55	0.35	0
	1.73	19.80	11.31	4.72	1.62	0.54	2.19	1.45
	(Failed)							
MUS	0.61	0	0	0	0	0	0	0
	0.79	1.60	0	0	0	0	0	0
	0.81	1.60	0.50	0	0	0	0	0
	1.30	1.26	0.76	0.33	0	0	0	0
	1.40	7.16	0.83	0.66	0	0	0	0
	1.56	17.6	5.86	0.36	0	0	0	0
	1.82	50.23	3.13	4.90	1.26	0.93	0.16	0
	(Failed)							

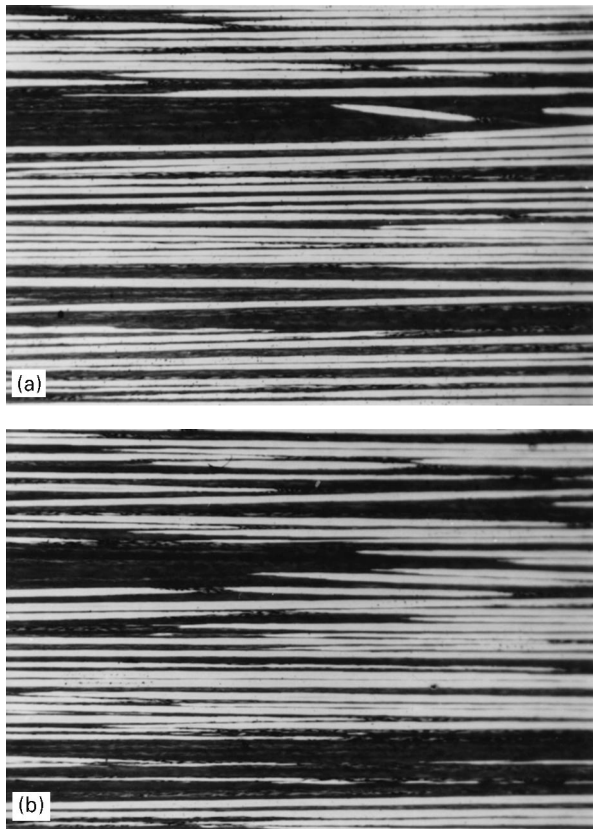


Figure 5 Photomicrograph of sectioned tow samples. (a) Sectioned MUS tow 1.65 GPa applied stress, (b) sectioned MEBS tow 1.7 GPa applied stress.

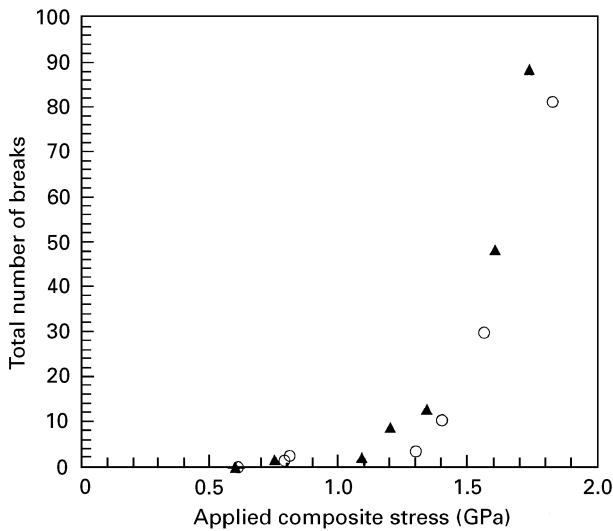


Figure 6 The cumulative number of filament breaks at each level of applied strain: (○) MUS, (▲) MEBS.

surface of the tow will have less of a weakening effect than those in the core resulting in higher failure stresses and a lower scatter in strength. There is also a small effect due to the thermal mismatch between the carbon and the glass fibre.

#### 4.2. Impregnated bundle failure mechanism

In the failed tow sections, the number of breaks per metre was found to be higher for the sized fibre tows.

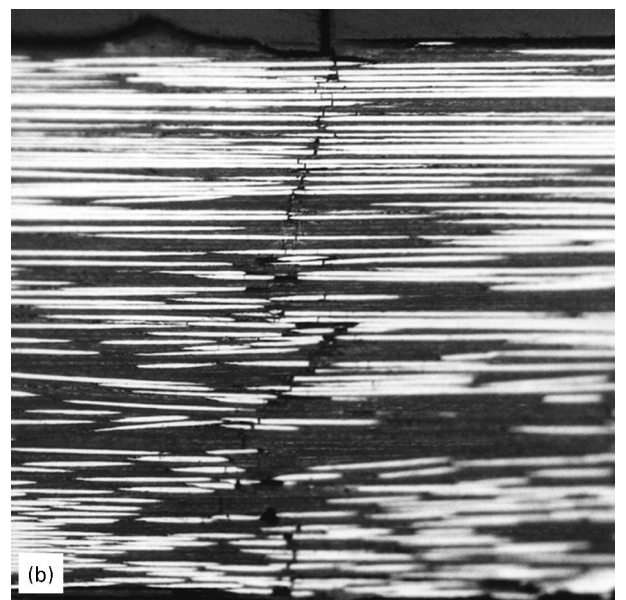
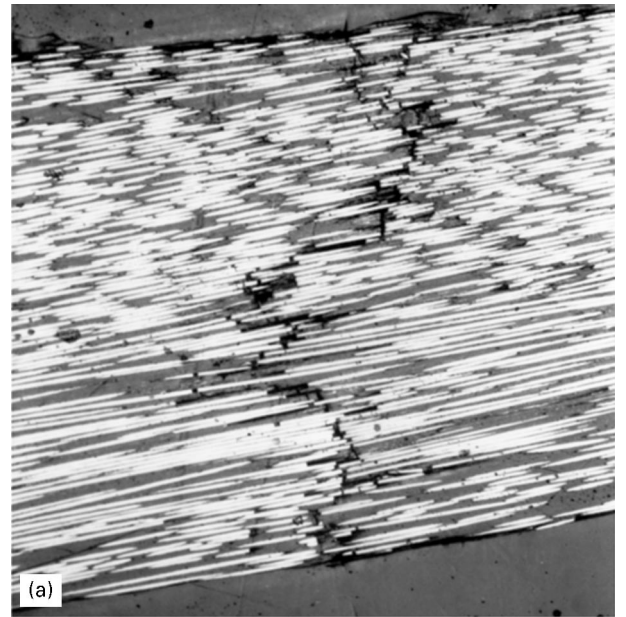


Figure 7 Photomicrograph of the failure zone of impregnated hybrid bundles. (a) MUS tow, (b) MEBS tow.

This phenomenon could be attributed to the number of *i*-plets observed with *i* greater than one higher for the sized tows. Prior to composite failure, the largest *i*-plet observed for the MUS tow was a two-dimensional 3-plet, whereas for the MEBS sample, a 6-plet was observed. At composite failure, the largest cluster observed was a two-dimensional 7-plet for the MEBS and a 6-plet for the MUS tows.

Work performed by Marston *et al.* [14] using laser Raman spectroscopy has mapped the fibre stress along the individual fibres around single and double fibre breaks within MUS and MEBS composite tows. Laser Raman spectroscopy is a relatively new technique that will allow the measurement of local load transfer at the interface between fibres and the matrix. A summary of the values of the stress concentration factors,  $K_r$ , interfacial shear stress ISS, ineffective lengths,  $\delta$ , and positive affected lengths, PALs, for single and double breaks in the surface of a sized and

TABLE III Summary of the recorded stress concentration factors,  $K_r$ , interfacial shear stress, ISS, ineffective lengths,  $\delta$ , and positive affected lengths, PALs, for a single break MUS and MEBS tow

Tow (sample)	$\delta$ ( $\mu\text{m}$ )	PAL ( $\mu\text{m}$ )	ISS (MPa)	Average $K_r$ for fibres given in parentheses		
				Interfibre distance 10.8 $\mu\text{m}$	Interfibre distance 21.7 $\mu\text{m}$	Interfibre distance 32.6 $\mu\text{m}$
MUS	220	220	21	(3 + 5) 1.14	(2 + 6) 1.04	(1 + 7) 1.0
MEBS	200	200	30	(3 + 5) 1.18	(2 + 6) 1.14	(1 + 7) 1.0
MUS				(3 + 6) 1.33	(2 + 7) 1.26	(1 + 8) 1.1
(Fibre 4)	220	220	24			
(Fibre 5)	220	220	20			
MEBS				(3 + 6) 1.18	(2 + 7) 1.1	(1 + 8) 1.07
(Fibre 4)	200	200	28			
(Fibre 5)	200	200	29			

unsized impregnated tow, are shown in Table III. Around a single fibre fracture the fibre stress on the failed fibre, in this case fibre number 4, as well as the three fibres situated either side on the same surface plane, (namely 6, 7, 8 and 1, 2, 3) were mapped using the laser Raman microprobe. For a double-fibre break, in this case fibres 4 and 5, the stress was mapped on the neighbouring fibres (fibres 1, 2, 3 and 6, 7, 8) over a short gauge length.

It is evident that, at the point of fibre fracture, a higher stress intensification is observed for the sized fibres as a result of a stronger interface bond. In the unsized fibres, the bond strength is lower resulting in a lower stress intensification distributed over approximately the same positive affected length (220  $\mu\text{m}$  for the MUS tow, 200  $\mu\text{m}$  for the MEBS tow). Thus in the case of the sized fibre, there is a greater probability of the increased stress in neighbouring fibres coinciding with a flaw leading to related failures in adjacent fibres. In the unsized fibres, there is a lower probability of stress intensification coinciding with a flaw in neighbouring fibres and hence a reduction in the number of related fractures or *i*-plets.

Fig. 7a and b show that in the case of the unsized tow the crack is seen to be more longitudinally extended along the fibre/matrix interface, whereas for the sized fibre the crack propagated almost perpendicular to the fibre direction. The unsized sample involved more debonding either side of the fracture path and this debonded region extended for approximately 1.5 mm from the break. In the case of the sized hybrid composite, little debonding was seen and the path of the crack was more longitudinal in nature, indicating a stronger interface.

#### 4.3. The effect of the interface strength upon composite failure

It has been shown that at fibre failure, the load that was originally carried by the fibre is redistributed into the remaining composite [14] where the matrix has the effect of localizing the redistribution of load to the neighbouring fibres. The rate of stress transfer is determined by the ratio of the fibre tensile modulus to the shear modulus of the matrix. The higher this ratio,

$E_f/G_m$ , the longer is the ineffective length,  $\delta$ , and the lower is maximum shear stress at the fibre end. If the matrix around the fibre and the interphase region is stiff (high  $G_m$ , lower ratio  $E_f/G_m$ ) then the stress transfers back into the broken fibres very quickly and the ineffective length is small in size. Thus the local stress concentration surrounding the filament break is higher because of the rapid nature of stress transfer in that region. Conversely, if the material surrounding the filament break is compliant (low  $G_m$ , higher  $E_f/G_m$ ) the ineffective length is large, because a large distance is required to transfer stress back into the broken fibre.

Thus, if the ineffective length is small and the stress concentrations are high there is a tendency for the neighbouring fibres to break, and the fracture propagates across the specimen in the region of the initial cluster. Close inspection of Fig. 7a shows initiation of failure appears to have started from a cluster of fibre breaks, shown at point A. This cluster can be regarded as a Griffith crack which remains stable until it achieves a critical size, where it causes unstable failure. However, in the case of a large ineffective length, it is proposed that fibre fractures will create a wider region of influence, and these regions will interact with other regions created by other fibre failures to cause linking together of the respective clusters of fibre breaks. This is the situation observed in Fig. 7b. Therefore, depending upon the properties of the fibre, the matrix and the interphase region, there is a tendency for the clustering of fibre breaks as a result of load redistribution around filament failures, or the tendency for fracture due to the statistical accumulation of defects in the sense of a bundle-strength concept.

#### 5. Conclusion

This work has demonstrated that the sizing of carbon fibres has a dramatic effect upon the mode of failure of a continuous fibre-reinforced composite. The sizing appears to reduce the strength of the composite tows by 7% and gives a more confined failure process, resulting in an overall 'brittle' failure mode. Hybrid bundles tested in tension confirm the existence of the hybrid effect, where the carbon fibre tow is stronger



when surrounded by a glass fibre-reinforced material. It was evident that the strength of the single filaments in air were relatively insensitive to the effects of fibre sizing.

A conflict of approach has been shown when trying to obtain the ultimate composite strength. One might, on the basis of "bundle strength" considerations, use a stiff interface and matrix to reduce the possibility of interaction of fibre fractures at different positions along the length of neighbouring fibres. However, if we consider stress concentration effects and the fact that brittle fracture is as a result of a propagating flaw in a direction transverse to the fibre axis, it would be beneficial to make the surrounding matrix and interface compliant to reduce this stress overload. This is a problem frequently encountered in the design of the optimum tensile strength in a composite material.

### Acknowledgements

One of the authors (C.M.), gratefully acknowledges the support of The Institute of Materials and The Royal Academy of Engineering which provided the opportunity to perform part of the experimental work presented here at the University of Southern California (USC). Professor Steven Nutt, USC, is thanked for hosting the visit. Jonas Neumeister, Swedish Aeronautical Research Institute (FFA), is also thanked for useful discussions. Dr Costas Galiotis College and other members of the Raman group at Queen Mary and Westfield College, University of London, are gratefully acknowledged for invaluable support,

encouragement, and the facilities for laser Raman spectroscopy experimentation.

### References

1. M. J. FOLKS and S. T. HARWICK, *J. Mater. Sci. Lett.* **6** (1987) 656.
2. M. GUIGON and E. KLINKLIN *Composites* **25** (1994) 534.
3. T. H. CHENG, J. ZHANG, S. YUMITORY, F. R. JONES and C. ANDERSON, *ibid* **25** (1994) 661.
4. S. YUMITORY, D. WANG and F. R. JONES, *ibid* **25** (1994) 698.
5. P. W. BARRY, *J. Mater. Sci.* **13** (1978) 2177.
6. W. WEIBULL, *J. Appl. Mech.* **18** (1951) 293.
7. A. S. WATSON and R. L. SMITH, *J. Mater. Sci.* **20** (1985) 3260.
8. P. FAVRE, F. SEVERINI and L. LANDRO, "Interfacial contribution to the temperature dependent properties of carbon fibre reinforced composites", 12 months Technical progress report, contract BREU/CT91-0503, Proposal No Be-4016-90 (1992).
9. ASTM 3379, "Tensile strength and Young's modulus for high modulus single-filament material", "*Book of ASTM Standards*", Vol. 7 (American Society for Testing and Materials, Philadelphia, PA, 1989) pp. 731-85.
10. S. B. BATDORF, *J. Reinf. Plast. Compos.* **1** (1982) 152.
11. C. H. ANDERSON and R. WARREN, *Composites* **15** (1984) 16.
12. F. W. ZOK, X. CHEN and C. WEBBER, *J. Am. Ceram. Soc.* **78** (1994) 1965.
13. M. BADER and S. B. BATDORF, "On the hybrid effect in carbon/glass fibre laminates", (1985), ECCM 1, Bordeaux.
14. C. MARSTON, B. GABBITAS, J. ADAMS, P. MARSHALL and C. GALIOTIS, *J. Compos. Mater.*, to be published.

*Received 21 May  
and accepted 2 July 1996*